Journal of Sound and Vibration (1997) **204**(2), 183–202

STRUCTURAL DAMPING IN LAMINATED BEAMS DUE TO INTERFACIAL SLIP

S. W. HANSEN

Department of Mathematics, Iowa State University, Ames, IA 50011, *U.S.A.*

AND

R. D. SPIES

Programa Especial de Matemática Aplicada PEMA, INTEC-CONICET, 3000 *Santa Fe, Argentina*

(*Received* 12 *March* 1996, *and in final form* 20 *December* 1996)

Three closely related models for two-layered beams in which slip can occur at the interface are described. In the first, beam layers are modelled under the assumptions of Timoshenko beam theory. Along the interface, an adhesive layer of negligible thickness bonds the surfaces so that a small amount of slip is possible. Friction is assumed to be proportional to the rate of slip. The second is obtained from the first by letting the shear stiffness of each beam tend to infinity. The third is obtained from the second by assuming that the moment of inertia parameter is negligible. In the last case, an analog of the Euler–Bernoulli beam is obtained which exhibits frequency proportional damping characteristics. The three models are compared, both numerically and analytically, and found to be in close agreement for low frequency motions. Optimal damping rates are calculated for these low frequency motions.

© 1997 Academic Press Limited

1. INTRODUCTION

In Hansen [1] a model for a two-layered plate in which slip can occur along the interface is derived. There, it is assumed that an adhesive layer of negligible thickness and mass bonds the two adjoining surfaces in such a way that the restoring force created by the adhesive is proportional to the amount of slip. The plate layers are modelled under the assumptions of Reissner–Mindlin plate theory, i.e., the straight filaments orthogonal to each center sheet at equilibrium remain straight during deformation and the transverse displacements are constant along each deformed filament. In the symmetric case, where both plates are identical, a system of bending equations can be decoupled from a set that describes the in-plane motions. These bending equations (see reference [1, equation (3.16)]) form a coupled hyperbolic system involving the transverse displacement, rotation angles and slips (i.e., the slip in two independent directions). This plate model reduces to the Reissner–Mindlin plate in the limit as the adhesive stiffness tends to infinity.

In this article we will be concerned with the beam analog, with strain-rate damping included, of the above described plate model [1, equation (3.16)]. The equations for this beam model in the absence of external forces are

$$\rho\ddot{w} + (G(\psi - w_x))_x = 0,$$
$$I_\rho(3\ddot{s} - \ddot{\psi}) - G(\psi - w_x) - (D(3s_x - \psi_x))_x = 0,$$
$$I_\rho\ddot{s} + G(\psi - w_x) + \tfrac{4}{3}\gamma s + \tfrac{4}{3}\beta\dot{s} - (Ds_x)_x = 0, \qquad (1a\text{–}c)$$

0022–460X/97/270183 + 20 $25.00/0/sv960913 © 1997 Academic Press Limited

where "˙" denotes differentiation with respect to time, the subscripted x denotes differentiation with respect to the longitudinal spatial variable, w denotes the transverse displacement, ψ represents the rotation angle, s is proportional to the amount of "slip" along the interface and the parameters ρ, G, I_ρ, D, γ, β are the density, shear stiffness, mass moment of inertia, flexural rigidity, adhesive stiffness and adhesive damping parameter, respectively (see section 2). The system (1) is an analog of the Timoshenko beam model in the sense that equations (1a, b) reduce exactly to the Timoshenko beam system if the slip s is assumed to be identically zero. The third equation describes the dynamics of the slip. A derivation of the system (1) with external forces included is given in section 2.

The authors' main interest in this article is to compare the spectral characteristics of system (1) with lower-order approximations for the case where the shear stiffness parameter G is large and the moment of inertia parameter I_ρ is small compared to D.

By letting $G \to \infty$ in the system (1) one obtains an analog of the Rayleigh beam, also involving an extra equation for the slip (see section 3). Then by setting $I_\rho = 0$ in the latter system one obtains the following:

$$\rho\ddot{\omega} - (D\xi_x)_{xx} = 0, \qquad \beta(\dot{\xi} + \dot{\omega}_x) + \gamma(\xi + w_x) - 3(D\xi_x)_x - \tfrac{3}{4}(Dw_{xx})_x = 0, \quad \text{(2a, b)}$$

where $\xi = 3s - \psi$ is the *effective rotation angle*. The spectral properties of equations (2) are analyzed in section 4.

To describe some of our results, first consider equations (2) in the undamped case, i.e., where $\beta = 0$. If the adhesive stiffness γ tends to infinity (effectively causing a no-slip condition between the two layers), then equation (2b) suggests that $\xi \approx -w_x$, so that equation (2a) reduces to the Euler–Bernoulli (EB) beam equation $\rho\ddot{w} + (Dw_{xx})_{xx} = 0$. On the other hand, if γ tends to zero (so that the two layers effectively become delaminated) then equation (2a) reduces to an EB beam with one fourth the stiffness of the case where $\gamma \to \infty$. (This is the same as the sum of the stiffnesses of two EB beams of thickness $h/2$.) For $\gamma > 0$ one finds that equations (2) predict a behavior which is intermediate between these two extremes, with high-frequency behavior approaching that of the case $\gamma = 0$.

If $\beta > 0$, the spectrum associated with system (2) consists of a sequence of negative real eigenvalues and a sequence of complex conjugate pairs which exhibit *frequency proportional damping*, that is, the real parts of the eigenvalues are approximately proportional to the imaginary parts. As the amount of damping in the adhesive layer is increased (i.e., as β increases), after some critical amount, the damping rates of the modes begin to decrease. Thus system (2) predicts an optimal level of damping, after which, adding more damping is counterproductive. The value of β that gives the optimal damping is given in proposition 4.1.

In section 5 the behavior of systems (1) and (2) is compared both analytically and numerically. One finds that equations (1) and (2) are in very close agreement provided that the frequency ω is small compared to G/ρ and ρ/I_ρ. In the example, a steel two-layer beam one meter long and one half centimeter thick is considered (see section 5). The spectrum associated with the two models agrees to within about one percent for the first twenty modes (up to about 15 KHz).

2. MODEL DESCRIPTION

The beam model we consider here coincides with a special case of the two-layer plate

model [1, equation (3.16)] when the composite plate consists of two identical rectangular plates of uniform thickness. Thus refer to reference [1] for a precise derivation of the model. Here, are outlined only the main points needed to derive the beam analog of the plate model in reference [1].

The laminated beam considered consists of two identical beams of uniform thickness $h/2$, width r and length l (see Figure 1). Assume that at equilibrium the upper and lower beams occupy the respective regions

$$Q^+ = \{(x, y, z) \in (0, l) \times (-r/2, r/2) \times (0, h/2)\},$$

$$Q^- = \{(x, y, z) \in (0, l) \times (-r/2, r/2) \times (-h/2, 0)\}.$$

2.1. KINEMATIC ASSUMPTIONS

Let $(U_1, U_2, U_3)(x, y, z)$ denote the displacement vector of the point which, when the beam is in equilibrium, has co-ordinates (x, y, z). (Any time dependence in this notation is suppressed). So that one may obtain a beam theory, all the displacements are assumed to be independent of the y co-ordinate, and the deformations are zero in the y direction:

$$\begin{cases} U_i(x, y, z) = U_i(x, 0, z), & i = 1, 3, \quad \forall (x, y, z) \in Q^+ \cup Q^-, \\ U_2(x, y, z) \equiv 0, & \forall (x, y, z) \in Q^+ \cup Q^-. \end{cases} \tag{3}$$

Since this beam model allows slip to occur along the interface, there will usually be a discontinuity in the displacement along the interface. Define u^+ and u^- by

$$u_i^{\pm}(x) = \lim_{z \to 0^{\pm}} U_i(x, y, z), \qquad i = 1, 3, \qquad \forall x \in (0, l).$$

Both the upper and lower beams will be modelled as Timoshenko beams which allow lontigudinal motions (i.e., stretching motions). Thus in each beam layer, planar cross-sections that at equilibrium are orthogonal to the centerlines of each beam are assumed to remain planar, but may translate transversely or longitudinally and also may rotate parallel to the y-axis. Furthermore, as is assumed in the Timoshenko theory, the transverse displacements are assumed to be constant throughout the deformed cross-sections.

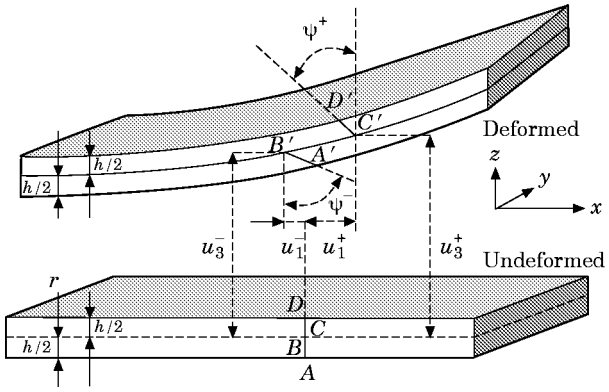

Figure 1. A cross-section through the points A, B, C, D and parallel to the y–z plane deforms independently in each layer into cross sections through A', B' in the lower layer and C', D' in the upper layer. The variables $\psi^{\pm}$, $u_1^{\pm}$ and $u_3^{\pm}$ are indicated. (No symmetries are assumed in this figure).

Thus the displacements are of the form

$$U_1(x, y, z) = \begin{cases} u_1^+(x) - z\psi^+(x), & \text{if} \quad (x, y, z) \in Q^+, \\ u_1^-(x) - z\psi^-(x), & \text{if} \quad (x, y, z) \in Q^-, \end{cases}$$

$$U_3(x, y, z) = \begin{cases} u_3^+(x), & \text{if} \quad (x, y, z) \in Q^+, \\ u_3^-(x), & \text{if} \quad (x, y, z) \in Q^-, \end{cases} \tag{4}$$

where $\psi^+(x)$ (respectively, $\psi^-(x)$) is the rotation angle, with positive orientation, through which the cross-section of the upper (respectively, lower) beam has rotated relative to its equilibrium position $(x, \cdot, \cdot)$ (see Figure 1).

So that the beams do not delaminate (in the transverse direction) one assumes that the transverse displacements of both beam layers are the same (and hence may be expressed in terms of a single transverse displacement variable w):

$$w = u_3^+ = u_3^- . \tag{5}$$

Implicit in equation (5) is a "small slip" assumption, namely, for equation (5) to be valid to linear order, the *interfacial slip* $u_1^+ - u_1^-$ should be small in comparison to h (see Figure 1).

Since the two beams are identical, as a consequence of conservation of momentum, the *bending motions* decouple from the *longitudinal motions* and possess the symmetry

$$U_1(x, y, z) = -U_1(x, y, -z), \qquad \forall (x, y, z) \in Q^+ \cup Q^- . \tag{6}$$

(The longitudinal motions satisfy $U_1(x, y, z) = U_1(x, y, -z)$ and $U_3 \equiv 0$). Thus, for the purpose of studying bending, equation (6) may be assumed *a priori*, and does not constitute a kinematic restriction. As a consequence of equation (6)

$$u_1^+ + u_1^- = 0, \qquad \psi^+ = \psi^- .$$

Let one denote

$$s = (u_1^+ - u_1^-)/2h, \qquad \psi = \psi^+ .$$

The *dimensionless slip* s is proportional to the interfacial slip $u_1^+ - u_1^-$. Note that $|s|$ should be small in comparison to 1 for consistency with the assumption (5).

It follows from equations (5) and (6) that for $(x, y, z) \in Q^+$, equation (4) may be rewritten as

$$U_1(x, y, z) = s(x)h - z\psi(x), \qquad U_3(x, y, z) = w(x). \tag{7}$$

Thus the displacement is uniquely determined in terms of the transverse displacement w, the *dimensionless slip* s and the *average rotation angle* ψ by equations (3), (5)–(7).

2.2. KINETIC AND POTENTIAL ENERGY OF BEAM LAYERS

Since the mass of the adhesive layer is assumed to be negligible, the kinetic energy is the sum of the kinetic energy of each beam:

$$\mathcal{K} = \frac{1}{2} \int_{Q^+ \cup Q^-} \rho(\dot{U}_1^2 + \dot{U}_2^2 + \dot{U}_3^2) \, \mathrm{d}Q,$$

where "˙" $= \partial/\partial t$ and $\rho = \rho(x) > 0$ is the volume density. Using equations (3), (5)–(7), one obtains

$$\mathscr{K} = \frac{hr}{2}\int_0^l [\rho(\dot{w})^2 + I_\rho((\dot{\psi} - 3\dot{s})^2 + 3\dot{s}^2)]\,\mathrm{d}x, \tag{8}$$

where $I_\rho = \rho h^2/12$.

The potential energy consists of the contribution from each beam and the adhesive. The potential energy for the beams is given in terms of the stresses σ_{ij} and strains ϵ_{ij} by

$$\mathscr{P}_b = \frac{1}{2}\int_{Q^+ \cup Q^-} \sum_{i,j=1}^{3} \sigma_{ij}\epsilon_{ij}\,\mathrm{d}Q.$$

Using equation (7) and small strain assumptions one obtains

$$\epsilon_{11} = \frac{\partial U_1}{\partial x} = s_x h - z\psi_x, \qquad \epsilon_{31} = \epsilon_{13} = \frac{1}{2}\left(\frac{\partial U_1}{\partial z} + \frac{\partial U_3}{\partial x}\right) = \frac{1}{2}(w_x - \psi).$$

(The other strains vanish due to equation (3) and the assumption that the transverse displacements are constant throughout the thickness). If the beam layers are homogeneous and transversely isotropic then

$$\sigma_{11} = E/(1 - \nu^2)\epsilon_{11}, \qquad \sigma_{31} = \sigma_{13} = 2G\epsilon_{13},$$

where E denotes the in-plane Young's modulus, ν represents the in-plane Poisson's ratio, and G represents the transverse shear modulus. In the isotropic case, $G = E/2(1 + \nu)$. We may allow E, G, ν to be x-dependent as long as they are assumed to be strictly positive and bounded with $\nu < \bar{\nu} < 1/2$.

Due to the symmetries in equations (5), (6) the strain energy of the upper and lower beams are the same, and thus from equation (7) we obtain

$$\mathscr{P}_b = \int_{Q^+}\left[\frac{E}{1 - \nu^2}(s_x h - z\psi_x)^2 + G(\psi - w_x)^2\right]\mathrm{d}z\,\mathrm{d}y\,\mathrm{d}x$$

$$= \frac{rh}{2}\int_0^l \{D[(\psi_x - 3s_x)^2 + 3s_x^2] + G(\psi - w_x)^2\}\,\mathrm{d}x, \tag{9}$$

where $D = Eh^2/12(1 - \nu^2)$ is the modulus of flexual rigidity (for a Timoshenko beam of thickness h, Young's modulus E and Poisson's ratio ν).

2.3. POTENTIAL ENERGY OF ADHESIVE LAYER

It is assumed that the thickness of the adhesive bonding the two plate layers is small enough so that the contribution of its mass to the kinetic energy of the entire beam may be ignored (or included in the beam layers).

To derive an expression for the potential energy carried by the adhesive, one *initially* assumes that the adhesive layer may be modelled as a Timoshenko beam of thickness d that is perfectly bonded to the beam layers (at $z = \pm d/2$). Assume that within this adhesive layer the following stress-strain law holds:

$$\sigma_{11} = E_a\epsilon_{11}, \qquad \sigma_{13} = 2G_a\epsilon_{13}. \tag{10}$$

By equation (6), the displacements within this thin layer are of the form

$$U_1(x, y, z) = z\theta(x), \qquad U_3(x, y, z) = w(x),$$

where θ is the rotation of a beam element. Since the total slip between the beam surfaces is $2sh$, for perfect bonding of the adhesive layer to the beam layers (at $z = \pm d/2$) one has

$$\theta = 2sh/d.$$

Therefore from small strain assumptions one obtains

$$\epsilon_{11} = \frac{2s_x hz}{d}, \qquad \epsilon_{13} = \epsilon_{31} = \frac{1}{2}\left(\frac{2sh}{d} + w_x\right).$$

The potential energy $\mathscr{P}_a$ of the adhesive layer is given by

$$\mathscr{P}_a = \frac{1}{2}\int_0^l \int_{-r/2}^{r/2} \int_{-d/2}^{d/2} \sum_{i,j=1,2,3} \sigma_{ij}\epsilon_{ij}\, \mathrm{d}z\, \mathrm{d}y\, \mathrm{d}x.$$

Performing the required integrations one obtains

$$\mathscr{P}_a = \frac{r}{2}\int_0^l \frac{dE_a h^2 s_x^2}{3} + dG_a\left(\frac{2sh}{d} + w_x\right)^2 \mathrm{d}x.$$

Now one uses the assumption that the adhesive layer is thin and compliant: one passes to the limit as $d \to 0$, $G_a \to 0$ with

$$\gamma := G_a h/d \qquad \text{fixed.} \tag{11}$$

In the limit one obtains

$$\mathscr{P}_a \to \frac{rh}{2}\int_0^l 4\gamma s^2\, \mathrm{d}x. \tag{12}$$

The limiting expression (12) for the potential energy of the adhesive layer can be viewed most simply as the potential energy obtained under the assumption that the adhesive supplies a restoring force proportion to the interfacial slip (i.e., Hooke's Law).

2.4. WORK

To fix ideas, assume that the beam is clamped at the end $x = 0$, subject to the volume distribution of body forces $(\tilde{f}_1(x, z), 0, \tilde{f}_3(x, z))$, and at the end $x = l$ is subject to the (area) distribution of forces $(\tilde{g}_1(z), 0, \tilde{g}_3(z))$. (The forces are assumed to be independent of y, with no forces acting in the y direction). The resultant force and moment density functions are defined as (for $i = 1, 3$)

$$f_i(x) = (1/rh)\int_A \tilde{f}_i\, \mathrm{d}S, \qquad g_i = (1/rh)\int_A \tilde{g}_i\, \mathrm{d}S, \qquad M_i(x) = (1/rh)\int_A \tilde{f}_i z\, \mathrm{d}S,$$

$$m_i = (1/rh)\int_A \tilde{g}_i z\, \mathrm{d}S, \qquad P_i(x) = (1/rh)\int_A \tilde{f}_i\, \mathrm{sgn}\,(z)\, \mathrm{d}S, \qquad p_i = (1/rh)\int_A \tilde{g}_i\, \mathrm{sgn}\,(z)\, \mathrm{d}S,$$

where $A = (-r/2, r/2) \times (-h/2, h/2)$ and $\mathrm{sgn}\,(z) = |z|/z$ denotes the sign function. The forces and moments f_1, M_3, P_3, g_1, m_1 and p_3 can produce no work due to the kinematic

assumptions in equations (4), (5) and the decoupling in equation (6). Thus, for consistency with these constraints one should assume that

$$f_1 = M_3 = P_3 = 0, \qquad g_1 = m_3 = p_3 = 0.$$

The work done by the remaining forces and moments on the plate is

$$\mathscr{W} = \int_{Q^+ \cup Q^-} (\tilde{f}_1 U_1 + \tilde{f}_3 U_3)\, \mathrm{d}Q + \int_{x=l} (\tilde{g}_1 U_1 + \tilde{g}_3 U_3)\, \mathrm{d}y\, \mathrm{d}z$$

$$= rh \int_0^1 (hsP_1 - \psi M_1 + wf_3)\, \mathrm{d}x + rh[hs(x)p_1 - \psi(x)m_1 + w(x)g_3]|_{x=l}.$$

2.5. EQUATIONS OF MOTION

The Lagrangian $\mathscr{L}$ on the interval $(0, T)$ is given by

$$\mathscr{L} = \int_0^T [\mathscr{K}(t) + \mathscr{W}(t) - \mathscr{P}_b(t) - \mathscr{P}_a(t)]\, \mathrm{d}t.$$

By the principle of virtual work, the equations of motion can be found by setting the variation of the Lagrangian to zero, where the variation is taken with respect to all kinematically admissible motions.

If one defines the *effective rotation angle* ξ by

$$\xi = 3s - \psi,$$

one obtains (see reference [2] for a similar calculation)

$$\rho\ddot{w} + (G\varphi)_x = f_3,$$

$$I_\rho\ddot{\xi} - G\varphi - (D\xi_x)_x = M_1,$$

$$I_\rho\ddot{s} + G\varphi + \tfrac{4}{3}\gamma s - (Ds_x)_x = \tfrac{1}{3}hP_1 - M_1, \tag{13a–c}$$

where

$$\varphi = 3s - \xi - w_x, \qquad 0 < x < l, \qquad t > 0.$$

The cantilever boundary conditions (obtained from the principle of virtual work) are

$$w(0) = \xi(0) = s(0) = 0, \qquad G(l)(3s(l) - \xi(l) - w_x(l)) = g_3,$$

$$D(l)\xi_x(l) = m_1, \qquad D(l)s_x(l) = \tfrac{1}{3}hp_1 - m_1, \qquad t > 0. \tag{14a–d}$$

Initial conditions may be given as

$$(\xi, s, w)|_{t=0} = (\xi^0, s^0, w^0), \qquad (\dot{\xi}, \dot{s}, \dot{w})|_{t=0} = (\xi^1, s^1, w^1), \qquad 0 < x < l. \tag{15}$$

Equations (13)–(15) are the beam analogs of the plate system [1, equations (3.16)–(3.18)]. A couple of comments are in order.

(1) If $\gamma \to \infty$ (so that the adhesive becomes infinitely stiff) one expects that $s \to 0$ (in some sense). Putting $s = 0$ in equations (13a) and (13b) results in the Timoshenko beam system. A precise statement of the convergence of solutions of the system (13)–(15) to those of the Timoshenko system is given in reference [1].

(2) If $\gamma = 0$ there is no coupling between the two beams other than applied forces. Thus (with appropriate initial conditions, boundary conditions and external forces) equations

(13)–(15) reduce to a system describing two uncoupled Timoshenko beams of thickness $h/2$. (Again, see reference [1] for a more detailed discussion).

2.6. DAMPING IN THE ADHESIVE LAYER

We will also be concerned with the effect of damping in the adhesive layer.

If the adhesive is modelled as a linear viscoelastic material then one replaces the stress-strain law in equation (10) by an appropriate viscoelastic constitutive law. Since the influence of direct stresses in the adhesive layer is not present in the limiting potential energy (12), one only needs to consider the stress-strain law for the transverse shear within the adhesive layer. The stress-strain law for the transverse shear (10) is modified to

$$\sigma_{13} = 2\int_0^t \tilde{G}_a(t-\tau)\dot{\epsilon}_{13}(\tau), \tag{16}$$

where $\tilde{G}_a$ is the relaxation modulus of shear. Note that equations (16) and (10) are the same if $\tilde{G}_a$ is constant. (It is assumed that the material is relaxed at time 0 in equation (16).)

According to the viscoelastic correspondence principle the equations of motion are modified in the same way that equation (10) is modified to equation (16) (see reference [2], for example). Therefore the equations of motion (13), (14) are modified by the substitution

$$\gamma s(x,t) \to \int_0^t \tilde{\gamma}(t-\tau)s(x,\tau)\,\mathrm{d}\tau, \tag{17}$$

where the relaxation function $\tilde{\gamma}(t)$ is defined in terms of the relaxation function $\tilde{G}_a$ by equation (11) (with γ and G_a replaced by $\tilde{\gamma}$ and $\tilde{G}_a$).

To simplify the present analysis it will be assumed for this article that $\tilde{\gamma}$ may be approximated by a linear combination of a constant function and an impulse at the origin:

$$\tilde{\gamma}(t) = \beta\delta(t) + \gamma.$$

This corresponds to a constitutive law of the form

$$\sigma_{13} = 2(G_a\epsilon_{13} + H_a\dot{\epsilon}_{13}), \tag{18}$$

where G_a and γ are related by equation (11) and H_a is similarly related to β. The damping obtained from equation (18) is referred to as *strain-rate* damping or *Kelvin–Voigt* damping and states the adhesive supplies a restoring force proportional to the rate of strain. In the limit as the thickness d of the adhesive layer tends to zero, β can be viewed as a coefficient of sliding friction for the interface between the beam layers.

Applying the correspondence principle one finds that the equations of motion (13) are modified to

$$\rho\ddot{w} + (G\varphi)_x = f_3, \qquad I_\rho\ddot{\xi} - G\varphi - (D\xi_x)x = M_1,$$
$$I_\rho\ddot{s} + G\varphi + \tfrac{4}{3}\gamma s + \tfrac{4}{3}\beta\dot{s} - (Ds_x)_x = \tfrac{1}{3}hP_1 - M_1, \tag{19a–c}$$

where

$$\varphi = 3s - \xi - w_x, \qquad 0 < x < l, \qquad t > 0.$$

The boundary conditions (14) and initial conditions (15) are unchanged. Note that the system (19) is the same as equation (1) in the absence of external forces.

It should be mentioned that if one is only interested in the forced response of the beam to harmonic inputs, the widely-used complex modulus approach (see reference [3] for a survey of this approach and many references) may be applied to model the viscoelastic adhesive layer. In this case equations (13) are modified by simply allowing γ to be complex. However this approach ignores any transient behavior and consequently cannot be used to study free motions or solutions of initial value problems.

3. LOW FREQUENCY APPROXIMATIONS

In this section two approximations of the system (19) which are valid for stiff and moderately thin beams are discussed. The first is obtained by letting the shear stiffness G tend to infinity in equation (19), while the second is obtained from the first by letting the moment of inertia parameter $I_\rho \to 0$.

3.1. LIMITING SYSTEM AS G$\to\infty$

If the shear stiffness G of the beam layers is large enough, the shear motions will usually be minimal and consequently a reasonable beam model should be obtained without allowing shear deformation.

In this subsection such a beam model is obtained as a limit as $G\to\infty$ of the original (shear deformable) model (19). For now, we proceed in a formal way. Justification will be provided in the next subsection.

First eliminating the term $(G\varphi)$ from two of the equations (19) and taking appropriate linear combinations of these equations and their derivatives, one obtains

$$\rho\ddot{w} + \tfrac{1}{4}(I_\rho\dddot{\xi})_x - \tfrac{3}{4}(I_\rho\ddot{s})_x - (\gamma s)_x - (\beta\dot{s})_x - \tfrac{1}{4}(D\xi_x)_{xx} + \tfrac{3}{4}(Ds_x)_{xx} = f_3 + (M_1 - hP_1/4)_x,$$

$$I_\rho(\dddot{\xi} + \ddot{s}) + \tfrac{4}{3}\gamma s + \tfrac{4}{3}\beta\dot{s} - (D(\xi_x + s_x))_x = \tfrac{1}{3}hP_1,$$

$$I_\rho(\dddot{\xi} - 3\ddot{s}) - 4G\varphi - 4\gamma s - 4\beta\dot{s} - (D(\xi_x - 3s_x))_x = 4M_1 - hP_1, \qquad (20a\text{–}c)$$

where

$$\varphi = 3s - \xi - w_x, \qquad 0 < x < l, \qquad t > 0.$$

Likewise, taking linear combinations of the boundary conditions in equation (14) and using equation (20c) at $x = l$ (to eliminate $G(l)\varphi(l)$ from the boundary condition (14b)) leads to

$$\xi(0) = w(0) = w_x(0) = 0,$$

$$[\tfrac{1}{4}I_\rho(\dddot{\xi} - 3\ddot{s}) - \gamma s - \beta\dot{s} - \tfrac{1}{4}(D(\xi_x - 3s_x))_x]_{x=l} = g_3 + M_1(l) - (h/4)P_1(l)$$

$$D(l)\xi_x(l) = m_1, \qquad D(l)(\xi_x(l) - 3s_x(l)) = 4m_1 - hp_1, \qquad t > 0. \qquad (21a\text{–}d)$$

As $G\to\infty$, by equation (9), finite energy solutions can exist only if the shear φ tends to zero. Setting $\varphi = 0$ in equations (20), (21) gives

$$\rho\ddot{w} - \tfrac{1}{4}(I_\rho\ddot{w}_x)_x - (\gamma s)_x - (\beta\dot{s})_x + \tfrac{1}{4}(Dw_{xx})_{xx} = f_3 + (M_1 - (h/4)P_1)_x,$$

$$I_\rho(4\dddot{\xi} + \ddot{w}_x) + 4\gamma s + 4\beta\dot{s} - (D(4\xi_x + w_{xx}))_x = hP_1, \qquad (22a, b)$$

where

$$s = \tfrac{1}{3}(\xi + w_x), \qquad 0 < x < l, \qquad t > 0,$$

with boundary conditions

$$\xi(0) = w(0) = w_x(0) = 0,$$

$$-\tfrac{1}{4}I_\rho(l)\ddot{w}_x(l) - \gamma(l)s(l) - \beta(l)\dot{s}(l) + \tfrac{1}{4}(Dw_{xx})_x(l) = g_3 + M_1(l) - (h/4)P_1(l),$$

$$D(l)\xi_x(l) = m_1, \qquad D(l)w_{xx}(l) = hp_1 - 4m_1, \qquad t > 0. \tag{23a–d}$$

Initial conditions for equations (22), (23) take the form

$$(\xi, w)|_{t=0} = (\xi^0, w^0), \qquad (\dot{\xi}, \dot{w})|_{t=0} = (\xi^1, w^1). \tag{24a, b}$$

The system (22)–(24) is (at least formally) the limiting form of the equations satisfied by (ξ, w) as $G \to \infty$. The convergence of the corresponding solutions is discussed in the next subsection.

Remark 3.1. The additional force terms in equations (22a) and (23b) (besides f_3, g_3) are due to moments applied to the individual layers. If the resultant applied moment in each beam vanishes (this does not rule out an overall applied moment) then $\tilde{f}_1$ satisfies

$$\int_{-h/2}^{0}\int_{-r/2}^{r/2}(z + h/4)\,\tilde{f}_1\,\mathrm{d}y\,\mathrm{d}z = \int_{0}^{h/2}\int_{-r/2}^{r/2}(z - h/4)\,\tilde{f}_1\,\mathrm{d}y\,\mathrm{d}x = 0, \qquad 0 < x < l.$$

A similar condition also applies to the surface force $\tilde{g}_1$. Under these conditions the moments M_1 and P_1 are no longer independent and are related by $hP_1 = 4M_1$, $hp_1 = 4m_1$, and consequently the additional forcing terms appearing in equations (22a) and (23b) vanish.

Remark 3.2. Equation (22) is closely related to the Rayleigh beam:

$$\rho\ddot{w} - (I_\rho\ddot{w}_x)_x + (Dw_{xx})_{xx} = 0. \tag{25}$$

If $\gamma \to \infty$ or $\beta \to \infty$ (so that the glue becomes infinitely stiff or viscous) it can be shown [1] that $s \to 0$ (weakly). Putting $s = 0$ in equation (20c) and combining this with equation (20a) gives equation (25). On the other hand if γ and β are zero then equation (22a) reduces to two uncoupled Rayleigh beams of thickness $h/2$ (as opposed to thickness h, as in equation (25)).

3.2. CONVERGENCE OF SOLUTIONS AS G$\to\infty$

The previous equations (22)–(24) are *formally* the limiting system as $G \to \infty$ of the system (14), (15) and (19). However, this does not necessarily imply any resemblance between corresponding solutions due to the presence of a boundary layer as $G \to \infty$. If equations (22)–(24) are meant to approximate a composite beam in which the shear moduli of the beam layers are large, then one would hope that solutions of equations (14), (15) and (19) become close (in some sense) to solutions of equations (22)–(24) as $G \to \infty$.

In this subsection, the sense in which solutions of equations (14), (15) and (19) converge to solutions of the limiting system (22)–(24) are described in a precise way. In order to do so, a few mathematical definitions and theorems one needed, which will be used solely in this subsection.

For simplicity the discussion is limited to the unforced problem with constant coefficients. (Similar results also hold for the forced problem with varying coefficients, but are more complicated to describe).

One first needs to describe the spaces of existence and uniqueness of finite energy solutions for the original system (14), (15) and (19) and the limiting system (22)–(24).

Let $L^2(0, l)$ denote the set of all square-integrable functions on the interval, $(0, l)$ and denote $H^n(0, l) = \{\varphi: \varphi, \varphi', \ldots, \varphi^{(n)} \in L^2(0, l)\}$. In the case of the cantilever boundary conditions (14) one lets

$$H^1_* = \{\varphi: \varphi \in H^1(0, l), \varphi(0) = 0\}$$

and defines the spaces

$$\mathscr{V} = (H^1_*)^3, \qquad \mathscr{H} = (L^2(0, l))^3.$$

Using [1, Theorem 4.1.], one can prove the following result.

Theorem 3.1. *Given any* $(\xi^0, s^0, w^0) \in \mathscr{V}$ *and any* $(\xi^1, s^1, w^1) \in \mathscr{H}$ *there is a uniquely defined solution* (ξ, s, w) *to the unforced problem* (14), (15), (19) *for which*

$$(\xi, s, w) \in C([0, \infty); \mathscr{V}) \cap C^1([0, \infty); \mathscr{H}). \tag{26}$$

Equation (26) states that the position variables vary continuously in time in the space $\mathscr{V}$ while the velocity variables vary continuously in time in the space $\mathscr{H}$. Since these spaces correspond to finite potential and kinetic energy, $\mathscr{V} \times \mathscr{H}$ is referred to as the *finite energy space* for equations (14), (15), (19).

Similar results are valid for the non-homogeneous problem provided the applied forces in equations (15) and (19) satisfy standard regularity conditions; see reference [2].

Now define $H^2_* = \{\varphi \in H^2(0, l): \varphi(0) = \varphi_x(0) = 0\}$ and denote

$$W = H^1_* \times H^2_*, \qquad V = L^2(0, l) \times H^1_*.$$

The space $W \times V$ is the finite energy space for equations (22)–(24). More precisely, one can prove (similar to reference [1, Theorem 5.3.]) the following result:

Theorem 3.2. *For the unforced problem* (22)–(24), *given any* $(\xi^0, w^0) \in W$ *and any* $(\xi^1, w^1) \in V$ *there is a unique solution* (ξ, w) *to equations* (22)–(24) *for which*

$$(\xi, w) \in C([0, \infty), W) \cap C^1([0, \infty), V).$$

Now consider a family of solutions $(\xi(G), s(G), w(G))$ to equations (14), (15), (19) corresponding to shear modulus G and a fixed set of initial data $(\xi^0, s^0, w^0, \xi^1, s^1, w^1)$ of finite energy. By Theorem 3.1, there is a uniquely defined solution for every G. The plan is to show that $(\xi(G), s(G), w(G))$ converges weakly to a limit $(\xi(\infty), s(\infty), w(\infty))$ and furthermore that $(\xi(\infty), s(\infty), w(\infty))$ is a solution of equations (22)–(24).

Since this program has been carried out for the analogous plate system in reference [1], only the main points are described here.

In order that the initial data have finite energy as $G \to \infty$ one needs to impose that $w^0 \in H^2_*$ and $w^1 \in H^1_*$ and furthermore that within each beam initially there is no shear, i.e.,

$$3s^0 = \xi^0 + w^0_x, \qquad 3s^1 = \xi^1 + w^1_x. \tag{27}$$

It follows from the fact that the unforced problem is dissipative that the energy $\mathscr{E}(t)$ remains bounded for all t in $[0, T]$ and for all G. It thus follows from equation (9) that the shear φ must tend to zero uniformly in t as $G \to \infty$. Furthermore, since the initial energy is independent of G (since equation (27) is imposed) one has (again, using that the energy is dissipative) that the $\mathscr{V} \times \mathscr{H}$ norms of the solutions are uniformly bounded independent of t and G. This implies the existence of a weak limit point as $G \to \infty$. It is then possible to show that this limit point is unique and is a solution of the limiting system (22)–(24).

More precisely, from reference [1] one has the following result.

Theorem 3.3. *Let* (ξ^0, w^0), (ξ^1, w^1) *be given in* $W \times V$ *and moreover assume that* s^0 *and*

s^1 *satisfy equation* (27). *Then for any* $T > 0$ *the solution* $(\xi(G), s(G), w(G))$ *to the unforced problem* (14), (15), (19) *tends to* (ξ, s, w) *as* $G \to \infty$ *in the sense that*

$$\begin{cases} (\xi(G), s(G), w(G)) \to (\xi, s, w) & \text{in } L^\infty(0, T, \mathscr{V}) \text{ weak-star}, \\ (\dot{\xi}(G), \dot{s}(G), \dot{w}(G)) \to (\dot{\xi}, \dot{s}, \dot{w}) & \text{in } L^\infty(0, T, \mathscr{H}) \text{ weak-star}, \end{cases}$$

where (ξ, w) *is the unique solution of equations* (22)–(24) (*with no external forces*) *and* $3s = \xi + w_x$.

The weak convergence in Theorem 3.3. is probably the best that can be expected since for each $G > 0$ "shear modes" will be present, and as the shear stiffness increases, these oscillations increase in frequency, but may not necessarily go to zero pointwise. In the limiting system these oscillations are eliminated through "averaging effects"; i.e., in much the same way that $\sin(Kx) \to 0$ (weakly) as $K \to \infty$.

3.3. LIMIT AS $I_\rho \to 0$

For the moment consider the Rayleigh beam (25). If I_ρ/ρ is very small then the EB beam obtained by setting I_ρ equal to 0 will provide a close approximation to equation (25) for the low frequency range of the spectrum. Of course this is not true for the higher frequencies since the principal symbols associated with equation (25) and the EB beam are different. In the same way, the system obtained by setting $I_\rho = 0$ in equations (22)–(24) will also be seen to provide a close approximation to equations (22)–(24) for the low frequencies.

Putting $I_\rho = 0$ in equations (22)–(24) gives

$$\rho\ddot{w} - (\gamma s)_x - (\beta \dot{s})_x + \tfrac{1}{4}(Dw_{xx})_{xx} = f_3 + (M_1 - (h/4)P_1)_x,$$
$$\beta \dot{s} + \gamma s - (D\xi_x + \tfrac{1}{4}Dw_{xx})_x = (h/4)P_1, \tag{28a, b}$$

where

$$3s = \xi + w_x, \qquad 0 < x < l, \qquad t > 0,$$

with boundary conditions

$$\xi(0) = w(0) = w_x(0) = 0,$$
$$-(\gamma(l)/3)(\xi(l) + w_x(l)) - (\beta(l)/3)(\dot{\xi}(l) + \dot{w}_x(l)) + \tfrac{1}{4}(Dw_{xx})_x(l) = g_3 + M_1(l) - (h/4)P_1(l),$$
$$D(l)\xi_x(l) = m_1, \qquad D(l)w_{xx}(l) = hp_1 - 4m_1, \qquad t > 0. \tag{29a–d}$$

The initial conditions may be specified as

$$w|_{t=0} = w^0, \qquad \dot{w}|_{t=0} = w^1, \qquad \xi|_{t=0} = \xi^0. \tag{30}$$

If $\beta = 0$ it is necessary to specify the compatibility condition

$$(\gamma/3)(\xi^0 + w^0) - [D(\xi^0_x + \tfrac{1}{4}w^0_{xx})]_x = M_1|_{t=0}. \tag{31}$$

A thorough investigation of the existence and uniqueness properties of equations (28)–(30) is beyond the scope of the present article. However, in the next section the spectrum of equations (28)–(30) in the case of constant coeficients and simply supported boundary conditions will be examined. For that case a unique solution is well defined through separation of variables.

The system (28), (29) can often be written in a simpler form. In particular, remark 3.1. concerning the terms $(M_1 - (h/4)P_1)_x$ in equation (28a) and similar terms in equations (29b) and (29d) still applies.

In the absence of all external forces equation (28) can be rewritten as

$$\rho\ddot{w} - (D\xi_x)_{xx} = 0,$$

$$(\beta/3)(\dot{\xi} + \dot{w}_x) + (\gamma/3)(\xi + w_x) - (D(\xi_x + \tfrac{1}{4}w_{xx}))_x = 0, \qquad 0 < x < l, \qquad t > 0, \quad (32a, b)$$

which is the same as equation (2). Thus, as mentioned in the introduction, equation (28) is closely related to the EB beam. This relationship is described in detail in the next section.

Other boundary conditions besides equation (29) are easily deduced from equation (29). For example, in the simply supported case there are no applied moments at the ends and the ends are fixed. If there are no applied moments on the interior then the simply supported boundary conditions take the form

$$w(i) = w_{xx}(i) = \xi_x(i) = 0, \quad i = 0, l, \qquad t > 0, \tag{33}$$

Remark 3.3. In the constant coefficient case (32) (or (28)) is also closely related to the sixth order beam model of DiTaranto [4] and Mead and Markus [5]. (These are both the same model; see reference [6].) If one begins with the three-layer model in reference [6], in the symmetric case (with the outer layers identical) and a center layer of thickness d and shear modulus K, then passes to the limit as $d \to 0$, $K \to 0$ with K/d fixed, one obtains a sixth order equation which is, under certain conditions, equivalent to equation (32). This only applies to the constant coefficient case with special boundary conditions and initial conditions that admit sinusoidal solutions.

4. SPECTRAL ANALYSIS

In this section the spectral characteristics of equations (32), (33) in the case of constant coefficients are analyzed. In this case, the eigenfunctions associated with equations (32), (33) are purely sinusoidal. Thus, to analyze the spectrum one assumes solutions to equations (32), (33) of the form

$$w = \mathrm{e}^{s_k t} \sin(\alpha_k x), \qquad \xi = B\,\mathrm{e}^{s_k t} \cos(\alpha_k x),$$

where $\alpha_k = k\pi/l$. Then the boundary conditions (33) are satisfied and equation (32) holds provided

$$\rho s_k^2 - BD\alpha_k^3 = 0, \qquad (\beta s_k + \gamma)(B + \alpha_k) + 3D\alpha_k^2(B + \alpha_k/4) = 0. \tag{34a, b}$$

Solving for B in equation (34a) and substituting this into equation (34b) gives

$$\beta\rho s_k^3 + (3D\alpha_k^2 + \gamma)\rho s_k^2 + \beta D\alpha_k^4 s_k + D\alpha_k^4(\gamma + 3D\alpha_k^2/4) = 0. \tag{35}$$

4.1. THE CASE $\beta = 0$

When $\beta = 0$ there are two roots $s_k = \sigma_k$ and $s_k = \bar{\sigma}_k$ to equation (35), where

$$\sigma_k = \mathrm{i}\sqrt{D\alpha_k^4(\gamma + 3D\alpha_k^2/4)/\rho(\gamma + 3D\alpha_k^2)}. \tag{36}$$

The *flexural wave speeds* are defined by $v_k = \sigma_k/(\mathrm{i}\alpha_k)$. If $\gamma \to \infty$ one sees from equation (36) that $v_k \to \alpha_k\sqrt{D/\rho}$, the same as in the EB beam $\rho\ddot{w} + Dw_{xxxx} = 0$. If $\gamma \to 0$ the wave speeds tend to half this value, the same as an EB beam with stiffness $D/4$. For fixed $\gamma > 0$ the wave speeds are between these two extremes, asymptotically approaching the values of the case $\gamma = 0$ as the frequency increases. Similar behavior of flexural wave speeds has been seen in sandwich plate theories [6]. Furthermore, the decrease in flexural wave speeds in comparison to that predicted by the EB theory for composite materials is also supported by experiments [7].

4.2. THE CASE $\beta \neq 0, \gamma = 0$

When $\beta > 0$, $\gamma = 0$, letting $v_k = -\alpha_k^2/s_k$, equation (35) becomes

$$(3D^2/4)v_k^3 - D\beta v_k^2 + 3D\rho v_k - \beta_\rho = 0, \tag{37}$$

or, equivalently $F(v_k) = 3D/\beta$, where

$$F(v) \doteq ((D/\rho)v^2 + 1)/v((D/4\rho)v^2 + 1).$$

By noting that F is an odd function with the properties: $F(v) \to +\infty$ as $v \to 0^+$, $F(v) \to 0$ as $v \to +\infty$, F is decreasing on $(0, \infty)$, it follows that equation (37) has only one real root $v = p$ which satisfies

$$\beta/3D < p < (4/3)/(\beta/D) \tag{38}$$

and a pair of complex conjugate roots, c, $\bar{c}$. By factoring out p one finds that

$$|c|^2 = 4\beta\rho/3pD^2, \qquad \sqrt{\rho/D} < \operatorname{Im} c < 2\sqrt{\rho/D}, \qquad \operatorname{Re} c = \tfrac{1}{2}(4\beta/3D) - p). \tag{39}$$

Furthermore,

$$p/\beta \to 1/3D, \qquad \operatorname{Im} c \to 2\sqrt{\rho/D}, \qquad \operatorname{Re} c \to 0 \qquad \text{as } \beta \to 0 \tag{40}$$

$$p/\beta \to 4/3D, \qquad \operatorname{Im} c \to \sqrt{\rho/D}, \qquad \operatorname{Re} c \to 0 \qquad \text{as } \beta \to \infty. \tag{41}$$

One thus finds that $s_k = -\alpha_k^2/v_k$, $(k = 1, 2, \ldots)$, and since the roots of equation (37) consist of c, $\bar{c}$ and p (independent of k), the eigenvalues associated with equations (32), (33) for the case $\gamma = 0$ consist of $\{\lambda_k(\beta)\} = \{\omega_k(\beta)\} \cup \{\sigma_k(\beta)\} \cup \{\bar{\sigma}_k(\beta)\}$,
where

$$\omega_k(\beta) = -k^2\pi^2/l^2 p(\beta), \qquad \sigma_k(\beta) = -k^2\pi^2/l^2 c(\beta), \qquad k = 1, 2, \ldots, \tag{42, 43}$$

where $p(\beta)$ and $c(\beta)$ satisfy equations (37)–(41).

There are several interesting things to note.

(1) For fixed $\beta > 0$ the branch $\{\sigma_k(\beta)\}$ tends to ∞ (as $k \to \infty$) along a ray (from the origin) in the left half of the complex plane. Thus the real and imaginary parts of $\sigma_k(\beta)$ are proportional, i.e., the damping is *frequency proportional* (see Figure 2). Previously known frequency proportional damping models include the *square root* model [8] and the *spatial hysteresis* model [9]. This type of damping is in agreement with experimental measurement in composite beams [7].

(2) The branch of eigenvalues $\{\omega_k(\beta)\}$ is due to the parabolic component in equation (32), (33). As $\beta \to 0$, each of these eigenvalues tends to ∞ along the negative real axis, while

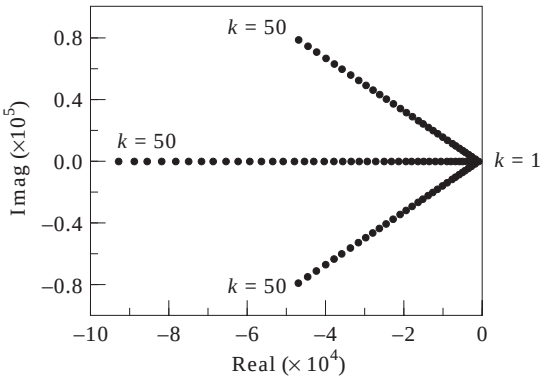

Figure 2. The three branches of eigenvalues for the model (32), (33) with $\gamma = 0$ (solutions of equation (35)).

as $\beta \to \infty$ they tend toward the origin. (Again, see Figure 2). This type of pattern, where there is a branch of negative real eigenvalues along with the vibrational eigenvalues is typical of thermoelastic systems as well as some viscoelastic beam models.

(3) By equations (40), (41), $c(\beta)$ tends to the imaginary axis in both extremes: as $\beta \to 0$ and as $\beta \to \infty$. Thus equation (43) indicates that all the eigenvalues tend to the imaginary axis as $\beta \to 0$ and also as $\beta \to \infty$. Thus the model (32), (33) suggests that there is an optimal level of damping achievable and beyond that point, adding more damping to the adhesive layer is counterproductive. This phenomenon has long been known to occur in composite beams involving damping layers [10]. Figure 3 illustrates the trajectories of the eigenvalues $\sigma_k(\beta)$. The value of β which gives the optimal damping is given in proposition 4.1.

Figure 2 shows the first 50 eigenvalues of equations (32), (33) for the case $\gamma = 0$, i.e., the roots of equation (35) for $k = 1, 2, \ldots, 50$. The parameters used are (all in MKS units) $\rho = 2000$, $D = 56\,250$, $l = 1$, $\beta = 22\,500$. The value of D was obtained by using $E = 2{\cdot}4 \times 10^{10}$ (a typical value for steel), $h = 0{\cdot}005$ and $v = 1/3$. The value of β was picked to give optimal damping (see proposition 4.1.). The following result concerning the problem of optimal damping of equations (32), (33) can be proved for the case $\gamma = 0$.

Proposition 4.1. *Let* $\sigma_k = \sigma_k(\beta)$, $k = 1, 2, \ldots$ *be the eigenvalues as defined by equation* (43). *Then* $\arg \sigma_k$ *is independent of* k *and*

$$\max_{0 \leqslant \beta < \infty} \arg \sigma_k(\beta) = 2\pi/3. \tag{44}$$

Furthermore, $\beta = 3\sqrt{D\rho/2}$ *is the unique value of* β *for which* $\arg \delta_k(\beta) = 2\pi/3$.

Proof. One knows by equation (43) that the argument of the eigenvalues σ_k, $k = 1, 2, \ldots$ are all the same and satisfy

$$\arg \sigma_k = -\arg(-c). \tag{45}$$

Note also that the values of $c(\beta)$, $0 \leqslant \beta < \infty$, together with the segment from $i\sqrt{\rho/D}$ to $2i\sqrt{\rho/D}$ form a continuous closed curve Σ in the closed right-half complex plane. Consider the points of intersection (if any) of Σ with the ray $R \doteq \{r\, e^{i\pi/3}: 0 \leqslant r < \infty\}$. If $v = r\, e^{i\pi/3} \in \Sigma \cap R$ then v satisfies equation (37), i.e.,

$$-3D^2r^3/4 - D\beta r^2\, e^{i2\pi/3} + 3D\rho r\, e^{i\pi/3} - \rho\beta = 0,$$

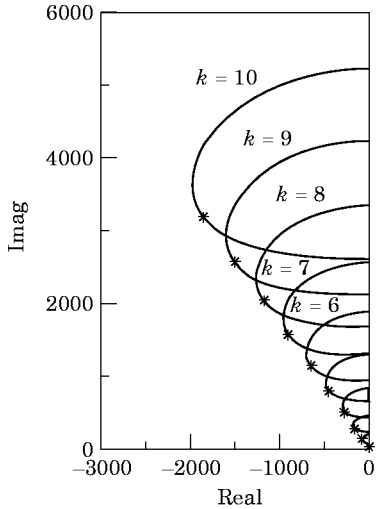

Figure 3. Trajectories of $\sigma_k(\beta)$ for $0 \leqslant \beta < \infty$, $1 \leqslant k \leqslant 10$, $\gamma = 0$ (equation (35)); points corresponding to the optimal damping $\beta = 3\sqrt{D\rho/2}$ are denoted by asterisks *.

which implies that $\mathrm{Im}\,(D\beta r^2\,e^{i2\pi/3}) = \mathrm{Im}\,(3D\rho r\,e^{i\pi/3})$ and therefore $r = 3\rho/\beta$. Plugging $v = (3\rho/\beta)\,e^{i\pi/3}$ into equation (37) results in $(9D\rho/(2\beta) - \beta)^2 = 0$ which implies $\beta = \beta^* = 3\sqrt{D\rho/2}$. Hence the ray R intersects the curve Σ only once at the point $c = c^*(\beta) = (3\rho/\beta^*)\,e^{i\pi/3} = \sqrt{2\rho/D}\,e^{i\pi/3}$. Since Σ encloses a bounded region of the complex plane, uniqueness of this intersection implies optimality; i.e., $\min_{0 \leqslant \beta < \infty} \arg c(\beta) = \arg c(\beta^*) = \pi/3$. Thus equation (44) follows from equation (45). □

Figure 3 shows the trajectories of the eigenvalues $\sigma_k(\beta)$, $1 \leqslant k \leqslant 10$, for $0 \leqslant \beta < \infty$. As β goes from zero to infinity the corresponding frequencies of each σ_k doubles. The values of ρ, D and l are the same as those used in Figure 2.

4.3. THE CASE $\gamma > 0$, $\beta > 0$.

Consider the case $\beta > 0$, $\gamma > 0$. From Rouché's Theorem applied to the polynomial in equation (35) one can deduce the following: If $\sigma_k(\gamma, \beta)$, $\bar{\sigma}_k(\gamma, \beta)$, $\omega_k(\gamma, \beta)$ denote the roots of the polynomial in equation (35), then

$$|\sigma_k(0, \beta) - \sigma_k(\gamma, \beta)|/|\sigma_k(0, \beta)| \to 0, \qquad \text{as } k \to \infty,$$

$$|\omega_k(0, \beta) - \omega_k(\gamma, \beta)|/|\omega_k(0, \beta)| \to 0, \qquad \text{as } k \to \infty,$$

that is, the stiffness of the adhesive does not significantly affect the position of the high frequency eigenvalues. It follows that all the conclusions reached for the case $\gamma = 0$ also hold (asymptotically) for the case $\gamma > 0$.

Figure 4 shows a comparison of the eigenvalues for the cases $\gamma = 0$ (same as in Figure 2) and the case $\gamma = 2{\cdot}0 \times 10^6$. This value of γ was picked using equations (11) with a typical value for a Young's modulus of a glue. Here $l = 10$ was used since with $l = 1$ the difference between the two branches was insignificant.

5. COMPARISON WITH THE GENERAL CASE $I_\rho > 0$, $0 < G < \infty$

In this section the spectrum of (19) is compared with the spectrum of (32) both analytically and numerically.

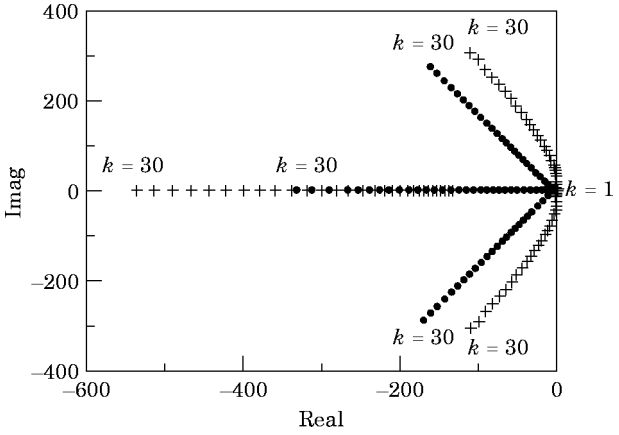

Figure 4. Comparison of the first 30 eigenvalues for the case $\gamma = 0$ ($\cdots$) and $\gamma = 2 \times 10^6$ ($+\ +\ +$) in the model (32), (33).

For the general unforced problem with simply supported boundary conditions and γ, D constant, system (19) takes the form

$$\rho\ddot{w} + G\varphi_x = 0, \qquad I_\rho\ddot{\xi} - G\varphi - D\xi_{xx} = 0, \qquad I_\rho\ddot{s} + G\varphi + \tfrac{4}{3}\gamma s + \tfrac{4}{3}\beta\dot{s} - Ds_{xx} = 0$$
$$\varphi = 3s - \xi - w_x, \qquad 0 < x < l, \qquad t > 0. \tag{46a–d}$$

The simply supported boundary conditions take the form

$$w(i) = \xi_x(i) = s_x(i) = 0, \qquad i = 0, l. \tag{47}$$

By letting $w = e^{s_k t}\sin(\alpha_k x)$, $\xi = B\cos(\alpha_k x)\,e^{s_k t}$ and $s = C\cos(\alpha_k x)\,e^{s_k t}$, where $\alpha_k = k\pi/l$, one obtains $\varphi = (3C - B - (k\pi/l))\cos((k\pi/l)\,x)\,e^{s_k t}$ and equations (46a–c) yield

$$\rho s_k^2 + G(k\pi/l)(k\pi/l + B - 3C) = 0,$$
$$I_\rho B s_k^2 - G(3C - B - k\pi/l) + DBk^2\pi^2/l^2 = 0,$$
$$I_\rho C s_k^2 + G(3C - B - k\pi/l) + \tfrac{4}{3}\gamma C + \tfrac{4}{3}\beta C s_k + DCk^2\pi^2/l^2 = 0. \tag{48a–c}$$

From equation (48a, b) one obtains

$$B = \frac{\rho s_k^2}{\alpha_k(I_\rho s_k^2 + D\alpha_k^2)}, \qquad C = \frac{\alpha_k}{3} + \frac{\rho s_k^2}{3\alpha_k}\left(\frac{1}{I_\rho s_k^2 + D\alpha_k^2} + \frac{1}{G}\right).$$

Putting these values of B and C into equation (48c) results in

$$\sum_{i=0}^{6} C_i s_k^i = 0, \tag{49}$$

where the coefficients C_i, $i = 1, \ldots, 6$ are given by

$$C_6 = 3\rho I_\rho^2/4G, \qquad C_5 = \beta\rho I_\rho/G,$$
$$C_4 = I_\rho[\rho(3 + \gamma/G) + \tfrac{3}{4}\alpha_k^2(I_\rho + 2\rho D/G)], \qquad C_3 = \beta(\rho + I_\rho\alpha_k^2 + \rho D\alpha_k^2/G),$$
$$C_2 = [\rho(\gamma + 3D\alpha_k^2) + I_\rho(\gamma\alpha_k^2 + \tfrac{3}{2}D\alpha_k^4) + (\rho D\alpha_k^2/G)(\gamma + \tfrac{3}{4}D\alpha_k^2)]$$
$$C_1 = D\beta\alpha_k^4, \qquad C_0 = \alpha_k^4 D(\gamma + \tfrac{3}{4}D\alpha_k^2). \tag{50}$$

Note that formally setting $I_\rho = 0$ and $1/G = 0$ in equations (49)–(50) results in precisely equation (35).

Since equation (49) is sixth order (for each k), there are three additional roots compared to the third degree polynomial in equation (35). These are due to the presence of rotational modes of vibration that are not present in the simplified model (32), (33). However, under the assumption that G is very large and I_ρ is very small, the size of the eigenvalues corresponding to these rotational modes are quite large. In section 5.1. it is shown that the low frequency eigenvalues associated with equations (46), (47) are closely approximated by corresponding eigenvalues associated with (32), (33).

Figure 5 shows the first 300 eigenvalues of equations (46), (47). Here $I_\rho = 0{\cdot}004166$, $G = 7{\cdot}5 \times 10^9$ and $\gamma = 2 \times 10^6$ are used. All the other parameters remain the same as those used in Figure 2. These values are consistent with those used in Figure 2 and $G = \kappa E/2(1 + \nu)$, where κ denotes a shear correction coefficient that is taken to be 5/6. Note that the first of each of these "rotational" eigenvalues (marked "$k = 1$", but away from the origin) are of the order of the 300th eigenvalue corresponding to modes that are present in the model (32), (33).

5.1. ASYMPTOTIC ANALYSIS OF EQUATIONS (46), (47) AS $I_\rho \to 0$, $G \to \infty$

Suppose that $I_\rho = \epsilon \hat{I}_\rho$, $G^{-1} = \epsilon \hat{G}^{-1}$, where ϵ is a small parameter and $\hat{I}_\rho$, $\hat{G}$, γ, β, ρ, D are all $\mathcal{O}(1)$, that is, much larger than ϵ, but much smaller than $1/\epsilon$ (some renormalization may be required for this hypothesis to apply).

Let $Q_k(s)$ denote the polynomial in equation (49) and let $P_k(s)$ denote the polynomial in equation (35) (both with s_k replaced by s). Let $\Gamma(z, R)$ denote the circle of radius R about the complex number z.

Proposition 5.1. *Assume there are numbers* ϵ, δ; $0 < \epsilon < \delta < 1/2$ *such that*

$$|\lambda_k| < \delta/\epsilon, \tag{51}$$

where λ_k *denotes a root of* P_k. *Then there exists* $M > 0$, *independent of* k, δ, ϵ, *such that* Q_k *has exactly one root inside* $\Gamma(\lambda_k, M\delta|\lambda_k|)$.

The proof of proposition 5.1. involves an application of Rouché's theorem to the polynomials P_k and Q_k and is given in Appendix A.

Proposition 5.1. states that if λ_k is an eigenvalue corresponding to the model (2) (so that λ_k is one of the numbers σ_k, $\bar{\sigma}_k$ or ω_k in equations (42), (43)), and k is small enough so that (51) holds, then there is a unique eigenvalue $\hat{\lambda}_k$ corresponding to the model (1) for which $|\lambda_k - \hat{\lambda}_k| < M\delta|\lambda_k|$. Thus (since M is independent of δ) the relative error in approximating $\hat{\lambda}_k$ by λ_k is of the order of δ. The constant M in proposition 5.1. can be computed explicitly and is a maximum of sums, products and ratios (but not differences) of the parameters $\hat{I}_\rho$, $\hat{G}$, ρ, D, γ, β.

Figure 6 shows a comparison of the first 30 eigenvalues of the models (46), (47) and (32), (33). The values of the parameters used here are the same as those used in Figure 5.

One may apply proposition 5.1. to the parameter values used in Figure 6 as follows. Each parameter is first renormalized in equation (46) by division by ρ. This results in new parameter values: $\rho = 1$, $D = 28{\cdot}125$, $G = 3{\cdot}75 \times 10^6$, $\gamma = 1000$, $I_\rho = 2{\cdot}08 \times 10^{-6}$, $\beta = 11{\cdot}25$. Observe that by taking $\epsilon = 10^{-6}$, $\delta = 0{\cdot}01$, Proposition 5.1 predicts a relative error of the order of 1% for $|\lambda_k| < 10^4$, i.e., up to 10 KHz, which is approximately the same as the actual relative error.

6. SUMMARY AND CONCLUSIONS

In this paper a model for a symmetric, two-layer beam that allows interfacial slip was derived which includes the effects of shear deformation and rotary inertia in each beam

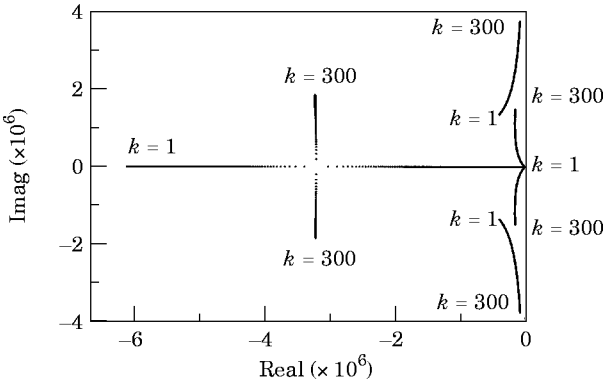

Figure 5. The six branches of eigenvalues obtained with the full model (46), (47) (solutions of equations (49), (50)).

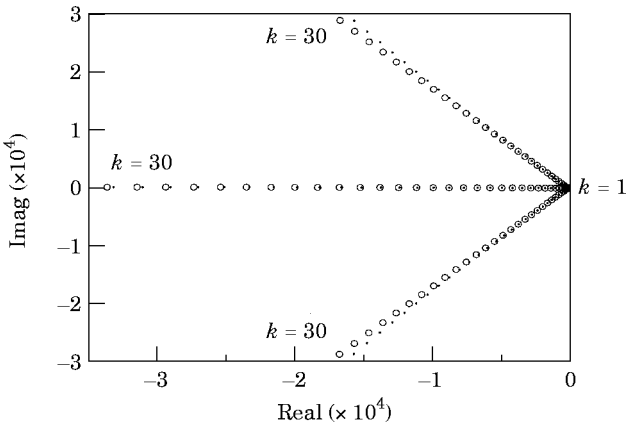

Figure 6. Comparison of the first 30 eigenvalues obtained with the full model (equations (49), (50)) and the limit case $I_\rho = 1/G = 0$ (equations (35), (42), (43)). Points marked · · · · correspond to the full model while points marked ○ ○ ○ are the roots of $P_k(s_k)$.

layer. The two layers were assumed to be bonded by a viscous adhesive of negligible mass and thickness. By letting the shear stiffness parameter G tend to infinity and dropping the terms involving the rotational inertia I_ρ, a much simpler model (28) is produced. If G is large and I_ρ is small then this simpler model provides a close approximation to the original model for harmonic motions with frequencies that are small compared to G and $1/I_\rho$. For these frequencies, the discussion in section 4 concerning the behavior of the spectrum and optimal damping also applies to the original model. It was found that the frictional damping resulted in a frequency-proportional damping pattern in the spectrum and the optimal damping angle was described in proposition 4.1.

This investigation was motivated towards understanding the damping characteristics in a multi-laminated or possibly fiber-composite beams. Here a single location where slip was possible was assumed, since this simplified the eigenvalue calculations. Future research will hopefully extend much of this analysis to beam models with many adhesive layers.

ACKNOWLEDGMENT

This research was supported in part by National Science Foundation grant DMS-9623144.

REFERENCES

1. S. W. Hansen 1994 In *Control and Estimation of Distributed Parameter Systems*: *Non-linear Phenomena* (editors W. Desch, F. Kappel, K. Kunish), International Series of Numerical Analysis, ISNA **118**, 143–170. Basel: Birkhaüser. A Model for a two-layered plate with interfacial slip.
2. J. E. Lagnese and J.-L. Lions 1989 *Modeling Analysis and Control of Thin Plates*, Recherches en Mathématiques Appliquées, RMA 6. New York: Springer-Verlag.
3. C. T. Sun and Y. P. Lu 1995 *Vibration Damping of Structural Elements*. Prentice Hall.
4. R. A. DiTaranto 1965 *Journal of Applied Mechanics* **32**, 881–886. Theory of vibratory bending for elastic and viscoelastic layered finite-length beams.
5. D. J. Mead and S. Markus 1969 *Journal of Sound and Vibration* **10**, 163–175. The forced vibration of a three-layer, damped sandwich beam with arbitrary boundary conditions.
6. D. J. Mead 1982 *Journal of Sound and Vibration* **83**, 363–377. A comparison of some equations for the flexural vibration of damped sandwich beams.

7. H. T. Banks, Y. Wang and D. J. Inman 1991 *AMSE J. Vibration and Acoustics* **116**, 188–197. Bending and shear damping in beams: frequency domain estimation techniques.
8. G. Chen and D. L. Russell 1982 *Quarterly of Applied Mathematics* **39**, 433–454. A mathematical model for linear elastic systems with structural damping.
9. D. L. Russell 1986 *Mathematical Models for the Elastic Beam and their Control—Theoretical Implications* (editors Brezis, Crandall and Kappel) series: Pitman Research Notes in Mathematics **152**, 177–216. Harlow: Longman Scientific and Technical.
10. D. Ross, E. E. Ungar, and E. M. Kerwin Jr. 1959 in *Structural Damping* (Section 3) The American Society of Mechanical Engineers, 49–85. Cambridge, MA: Bolt, Beranek and Newman Inc; Damping of Plate Flexural Vibrations by Means of Viscoelastic Laminates.

APPENDIX A: PROOF OF PROPOSITION 5.1

The polynomial Q_k may be written as

$$Q_k(s) = P_k(s) + \epsilon F_k(s) + \epsilon^2 G_k(s) + \epsilon^3 H_k(s).$$

The result follows from Rouché's theorem if the following inequality can be proved:

$$|P_k(s)| > \epsilon|F_k(s)| + \epsilon^2|G_k(s)| + \epsilon^3|H_k(s)|, \qquad \forall s \text{ on } \Gamma(\lambda_k, M\delta|\lambda_k|). \tag{A1}$$

There are two possibilities: either λ_k is a real root ω_k of equation (33) or it is one of the complex roots σ_k, $\bar{\sigma}_k$. Both cases are handled in the same way so consider only the case $\lambda_k = \sigma_k$.

Let $R < |\sigma_k|/2$. Since $P_k(s) = \beta\rho(s - \sigma_k)(s - \bar{\sigma}_k)(s - \omega_k)$ and $\arg \sigma_k \leqslant 2\pi/3$ (see proposition 4.10) it follows from simple geometry that

$$|P_k(s)| \geqslant \beta\rho R\sqrt{3}/2|\sigma_k|^2(\sqrt{3} - 1)/2 > 0{\cdot}3\beta\rho|\sigma_k|^2 R \qquad \text{on } \Gamma(\sigma_k, R). \tag{A2}$$

To obtain an appropriate bound for the right side of equation (A1) one treats each term separately. For example, using equation (51) one has

$$\epsilon^3|H_k(s)| = |(3\rho\hat{I}_\rho^2/4\hat{G})\epsilon^3 s^6| \leqslant M_1\delta^3|\sigma_k|^3 \qquad \text{on } \Gamma(\sigma_k, R),$$

where $M_1 = (3\rho\hat{I}_\rho^2/4\hat{G})(3/2)^3$. The term $F_k(s)$ in equation (A1) is of the form

$$F_k(s) = \tilde{c}_2 s^2 + \tilde{c}_3 s^3 + \tilde{c}_4 s^4.$$

The term $\tilde{c}_2 s^2$ is the most troubling since $\tilde{c}_2 = 3\hat{I}_\rho D\alpha_k^4/2 +$ l.o.t., where l.o.t. denotes lower order terms in k. One has

$$|\tilde{c}_2 s^2| \leqslant M_2\alpha_k^4|\sigma_k|^2 \leqslant M_3|\sigma_k|^4 \qquad \text{on } \Gamma(\sigma_k, R).$$

Handling the other terms in the same way,

$$\epsilon|F_k(s)| \leqslant M_4\delta|\sigma_k|^3 \qquad \text{on } \Gamma(\sigma_k, R).$$

Likewise one can obtain a similar bound for $\epsilon^2|G_k(s)|$ on $\Gamma(\sigma_k, R)$.

Thus one obtains

$$\epsilon|F_k(s)| + \epsilon^2|G_k(s)| + \epsilon^3|H_k(s)| < M_5\delta|\sigma_k|^3 \qquad \text{on } \Gamma(\sigma_k, R), \tag{A3}$$

for any $R \leqslant |\sigma_k|/2$. Thus equation (A1) follows from equations (A2), (A3) provided $M_5\delta|\sigma_k|/(0{\cdot}3\beta\rho) < R \leqslant |\sigma_k|/2$. Thus by choosing δ sufficiently small, equation (A1) follows. On the other hand, Proposition 5.1. becomes trivial if one restricts δ to any interval of the form $[\delta_0, 1/2]$, by taking $M = 2/\delta_0$. □